Article:

Kumar, A. and De Souza, M.M. orcid.org/0000-0002-7804-7154 (2018) Impact of channel thickness on the performance of an E-mode p-channel MOSHFET in GaN. Applied Physics Letters, 112 (15). 153503. ISSN 0003-6951

https://doi.org/10.1063/1.5021306

Impact of channel thickness on the performance of an E-mode p-channel MOSHFET in GaN

Ashwani Kumar,[1] and Maria Merlyne De Souza[1,a)]

[1]*Department of Electronic and Electrical Engineering, University of Sheffield, George Porter Building, Broad Lane, Sheffield, S3 7HQ, UK*

Introduction of positive polarization charge by utilising an AlGaN cap layer between the gate oxide and channel is one of the promising techniques to deplete a two-dimensional hole gas (2DHG) to achieve an E-mode p-channel GaN MOSHFET. Results from TCAD simulations indicate that the off-state leakage increases by orders of magnitude for channel layers thicker than 20 nm in this structure. Biasing the two-dimensional electron gas (2DEG) beneath the 2DHG helps alleviate this limitation at the cost of reducing on-current. Scaling the access regions and combining the two techniques allows maximum benefit in terms of on-state current, negative threshold voltage and on/off current ratio.

The inherent 2DEG at an AlGaN/GaN interface of density in excess of $10^{13}\ cm^{-2}$ and mobility in excess of $1700\ cm^2/Vs$[1,2], coupled with a high breakdown field strength ($V_{br} > 2\ MV/cm$), is currently facilitating the next electronic revolution in high frequency and power applications.[3–5] When an additional GaN layer is grown on top of the AlGaN buffer in a conventional HEMT structure, a polarisation induced 2DHG is formed at its upper interface.[6] Reported values of the mobility of holes in this 2DHG at room temperature has not exceeded $43\ cm^2/Vs$[7] with an average of $\sim 16\ cm^2/Vs$ [8–10], much lower than even the $80\ cm^2/Vs$ at $1\ MV/cm$ in silicon.[11] Nevertheless, a combination of both 2DHG as well as a 2DEG has significant potential for GaN based complementary integrated circuits,[12] for power conversion in the Megahertz range.[13]

Achieving p-type E-mode operation with a sufficiently large negative threshold voltage requires depleting the 2DHG at zero gate bias, bringing about conflicting requirements of the substrate for power devices on the power management IC platform. The commonly known approaches to achieve E-mode operation of p-channel devices in GaN include a recessed gate.[13–15] However, this leads to a severe trade-off between the on-current, on/off ratio and threshold voltage in the device. Achieving a $|V_{th}| > |-2\ V|$ (for example in fail-safe applications such as automotive), via recessed gate alone, requires the thickness of the oxide and GaN channel layers to be reduced to $\sim 5\ nm$ for an AlGaN barrier with Al mole fraction of $18\ \%$,[16] leading to challenges in manufacturing and reliability. In an alternate approach, the polarization charge introduced by the AlInGaN (or AlGaN) barrier layer can be reduced by adjusting the mole fraction of the component materials.[7] This approach has been shown to yield a high on-off current ratio of $\sim 10^8$. Despite this fact, the on-current density is seen to be only $\sim 0.3\ mA/mm$ at a V_{th} of $\sim -1.5\ V$. Moreover, a reduction in the polarisation charge also leads to a reduction in density of the 2DEG, thus affecting the performance of other n-channel devices on the platform. In the approach from R. Chu *et al.*,[13] the GaN layer beneath the AlGaN barrier that contains the 2DEG is etched away, and AlGaN/GaN layers regrown to generate a 2DHG layer for p-type conduction. On the other hand, A. Nakajima *et al.*[17] use a bias voltage on the underlying 2DEG to modulate the threshold voltage of a p-channel device. This helps to obtain saturated $I_{DS} - V_{DS}$, since non-saturated $I_{DS} - V_{DS}$ characteristics are observed with a floating 2DEG. We have earlier examined an alternative approach to eliminate the 2DHG under the gate[16] that utilises regrowth of an AlGaN cap[18] for implementing a high performance normally-off p-channel MOSHFET.[19,20] In this work,

---

[a)] Author to whom correspondence should be addressed. Electronic mail: m.desouza@sheffield.ac.uk we evaluate the limits of capability of such a p-channel MOSHFET in GaN when integrated with power devices for power converter on a chip. We use simulations to analyse the benefits of a combination of techniques to achieve an optimum device performance, despite limitations of the poor mobility of holes. A modified AlGaN cap device with a biased 2DEG is proposed in this work, to aid the operation of the AlGaN cap in depleting the 2DHG under the gate and thus extend the performance of this technology.

Figure 1 (a) shows the schematic of the E-mode p-channel MOSHFET that utilises an additional AlGaN cap layer of 5 nm thickness regrown between the oxide and GaN channel in the gated region. The AlGaN cap layer introduces a positive polarization charge σ_{cap} at its interface with the GaN channel that counterbalances the negative polarization charge $-\sigma_P$ introduced by the AlGaN barrier at its bottom interface with the GaN channel layer. σ_{cap} can be controlled by adjusting the Al mole fraction in the AlGaN cap, x_{cap}, to deplete the 2DHG in the channel region under the gate, thereby enabling normally-off operation. The positive polarization charge has an added benefit of increasing the threshold voltage $|V_{th}|$ with increase in oxide thickness. This is opposite to the behaviour in a conventional p-channel MOSHFET in GaN, where a thinner oxide is required for more negative threshold voltage resulting from a reversal in the direction of the electric field inside the gate oxide.[16]

Figure 1 (b) shows the modified device examined in this work, which features an additional contact for applying a suitable bias over the 2DEG. A biased 2DEG assists the AlGaN cap to effectively suppress the 2DHG under the gate, thereby reducing the off-state leakage in E-mode operation. In both structures we consider a p-GaN/GaN/AlGaN/GaN stack as the baseline heterostructure that, from top to bottom (along $[000\bar{1}]$), consists of $20\,nm$ Mg-doped p-GaN, $20\,nm$ undoped GaN, $47\,nm$ AlGaN barrier with Al mole fraction of 23%, and a $1.5\,\mu m$ GaN buffer on a substrate. Al_2O_3 is used as a gate oxide with a thickness of $20\,nm$, while the gate length L_G is kept fixed at $0.25\,\mu m$. The lengths of the access regions between source and gate L_{SG} and gate and drain L_{GD} are initially kept at $1\,\mu m$, unless specified otherwise.

All the results are obtained from simulations implemented in Silvaco TCAD,[21] via a model as first introduced in [16,20], which has been calibrated to match experimental results reported in Reference [14]. In this model, the hole transport is modelled via field dependence of the mobility with a maximum value of $16\,cm^2/Vs$.[22] A charge density of $2.8 \times 10^{12} cm^{-2}$ and a trap density of $2.5 \times 10^{-12} cm^{-2}$ at the interface of the oxide/GaN, and a contact resistance ρ_c of $10^{-4}\,\Omega cm^2$ at the source and drain contacts to p-GaN are assumed. This value of ρ_c agrees with the average contact resistance reported for the ohmic contacts to p-GaN.[23]

The transfer characteristics of a p-channel device with grounded 2DEG (Figure 1 (a)), at different channel thicknesses, t_{ch}, are displayed in Figure 2 (a). Here, x_{cap} is adjusted such that the threshold voltage remains at $-2\,V$ irrespective of t_{ch}, as shown in the inset. An increase in x_{cap} is required at higher t_{ch} which reduces the density of 2DHG under the gate and leads to reduction in the on-state current $|I_{ON}|$ (defined as $|I_{DS}|$ at $V_{GS} = V_{DS} = -5\,V$) from its maximum value of $35\,mA/mm$, as shown in the inset (Figure 2 (a)). Moreover, the off-state current $|I_{OFF}|$ ($|I_{DS}|$ at $V_{GS} = 0, V_{DS} = -5\,V$) at zero gate bias in the transfer characteristics shows an increase by orders of magnitude with increase in t_{ch}.

This behaviour can be understood by analysing the band diagrams at two different thicknesses of channel layer, as shown in Figure 2 (b). For a thinner channel ($14\,nm$), the band bending introduced by σ_{cap} adequately maintains the valence band at the interface of the GaN channel and AlGaN barrier layer sufficiently below the Fermi level, resulting in a depletion of holes along this interface. However, for a thicker channel an additional $e^-\,QW$ develops at the top interface of the GaN channel where an increase in x_{cap} no longer has any impact in further lowering the valence band in the channel. Thus as the channel layer becomes thicker, the valence band at the GaN and AlGaN barrier interface comes close to the Fermi level as observed for $t_{ch} = 20\ nm$. This leads to a finite density of holes at this interface, responsible for an increase in the off-state current. Owing to this mechanism, the device produces an ideal on/off ratio of 10^{11} for thicknesses of the channel layer $< 18\ nm$. This channel thickness sets a limit upon its manufacturability, arising from the difficulty in controlling the diffusion of Mg ions[24] from the doped p-GaN layer that is required to form the ohmic contacts to the source and drain. The presence of the diffused Mg ions in the GaN channel layer would contribute to an increase in leakage current and mobility degradation from Coulomb scattering that are not accounted in these simulations, but would, in practise, make the device difficult to realise. Moreover, achieving a precise channel thickness via etching is also not preferable due to the difficulty in reliably reproducing etching depth with uniform surface.[25,26]

Our modified device with an additional base contact to the 2DEG (Figure 1 (b)) overcomes the restrictions imposed by channel thickness. In the modified device, an application of a suitable potential to the underlying 2DEG, V_B can be used as an additional handle in modulating the density of the 2DHG in the channel across the AlGaN barrier. Since the technology to contact the 2DEG is already well established in commercial n-channel GaN devices, the present device is more favourable in terms of manufacturability. It clearly avoids the problems associated with the manufacturing of undoped GaN channel layers with overlying Mg doped contact regions to problematically small values ($< 18\ nm$). The transfer characteristics of this device as plotted in Figure 3 reveal that $|I_{OFF}|$ can be suppressed with an increase in V_B, even with a thicker channel ($\approx 30\ nm$) and a lower x_{cap} (10 %). An increase in V_B helps lower the threshold voltage below zero, driving the device towards E-mode. However, the on-current of the device shows a sharp decrease with V_B, dropping to $\sim 15\ mA/mm$, half of its original value, as V_{th} changes from $0\ V$ to $-2\ V$, as shown in the inset.

The high sensitivity of the on-current to V_B arises from a distinction in the way in which the density of the hole gas is affected by the biased 2DEG in comparison to the AlGaN cap. Figures 4 (a) and (b) reveal the behaviour of the density of the 2DHG with respect to x_{cap} and V_B in different regions of the device. Since the AlGaN cap layer only resides under the gate, a change in x_{cap} only affects the density in the gate region, whereas the density in the access regions remains unaffected, as seen from Figure 4 (a). A biased 2DEG behaves as a secondary gate for the 2DHG, which acts across the AlGaN barrier, thereby affecting the density of 2DHG in both channel and access regions, as observed in Figure 4 (b). This reduction in the density of the 2DHG in the access region increases the resistance of the source to drain path, which results in the observed decrease in $|I_{ON}|$ with V_B.

One way to reduce the sensitivity of $|I_{ON}|$ with V_B and lower the impact of resistance introduced by the access regions is to minimise the lengths of the access regions. Figure 5 shows the transfer characteristics of an optimum device, where the lengths of both the access regions between the source and gate and gate and drain are kept at $300\ nm$.The inset shows a comparison of the transfer characteristics of this device with a change in trap charge density $\sigma_{cap/GaN}$ at the interface between the AlGaN cap and GaN channel. Owing to a reduction in the resistance of the access regions, the present device shows a maximum drain current of $28\ mA/mm$ at a $V_{th} = -2\ V$, which is almost double that achieved for a device with longer access regions ($L_{SG} = L_{GD} = 1\ \mu m$) in Figure 3. Despite a thicker channel of $30\ nm$, the on-off current ratio of the device is maintained at 10^8 (black curve with square symbols in the inset), a 4 order of magnitude gain over a device utilising only an AlGaN cap and a thinner channel of $20\ nm$ (see Figure 2). A higher on-state current is also the result of a higher x_{cap} and a lower V_B in contrast with the device in Figure 3, where an x_{cap} of 10 % and V_B of $5.5\ V$ is used for the same threshold voltage. A higher x_{cap} coupled with smaller V_B tends to favour the localised depletion of 2DHG under the gate rather than in the entire source to drain path.

As shown in the inset, the trap density at the AlGaN cap/GaN channel needs to be kept at minimum such that the variation in $\sigma_{cap/GaN}$ owing to the presence of traps is maintained well below $7 \times 10^{11} cm^{-2}$ to not significantly affect the device characteristics.

In conclusion, we have discussed potential solutions for achieving an E-mode p-channel device in GaN, necessary for a CMOS based power convertor in a Power Management Integrated Circuit (PMIC). Our analysis reveals that the technology employing an AlGaN cap is best suited for realising E-mode operation with highest on-current, yet it suffers from a high off-state current as the thickness of the channel is increased to 20 nm. Introducing an additional contact bias to the 2DEG acts as a secondary gate for controlling the density of 2DHG in the channel. This mechanism coupled with the AlGaN cap effectively eliminates the problem of higher off-state current observed at a thicker channel layer while still promising a higher on-current.

This work was partially funded by ENIAC-JU project E2SG under grant contract number 296131.

[1] M. Shur, B. Gelmont, and M. Asif Khan, J. Electron. Mater. **25**, 777 (1996).

[2] R. Oberhuber, G. Zandler, and P. Vogl, Appl. Phys. Lett. **73**, 818 (1998).

[3] U.K. Mishra, Shen Likun, T.E. Kazior, and Yi-Feng Wu, Proc. IEEE **96**, 287 (2008).

[4] D. Shibata, R. Kajitani, M. Ogawa, K. Tanaka, S. Tamura, T. Hatsuda, M. Ishida, and T. Ueda, in *2016 IEEE Int. Electron Devices Meet.* (IEDM, 2016), p. 10.1.1-10.1.4.

[5] O.I. Saadat, J.W. Chung, E.L. Piner, and T. Palacios, IEEE Electron Device Lett. **30**, 1254 (2009).

[6] A. Nakajima, K. Adachi, M. Shimizu, and H. Okumura, Appl. Phys. Lett. **89**, 193501 (2006).

[7] B. Reuters, H. Hahn, A. Pooth, B. Holländer, U. Breuer, M. Heuken, H. Kalisch, and A. Vescan, J. Phys. D. Appl. Phys. **47**, 175103 (2014).

[8] A. Nakajima, P. Liu, M. Ogura, T. Makino, K. Kakushima, S. Nishizawa, H. Ohashi, S. Yamasaki, and H. Iwai, J. Appl. Phys. **115**, 153707 (2014).

[9] P. Kozodoy, M. Hansen, S.P. DenBaars, and U.K. Mishra, Appl. Phys. Lett. **74**, 3681 (1999).

[10] A. Nakajima, P. Liu, M. Ogura, T. Makino, S. Nishizawa, S. Yamasaki, H. Ohashi, K. Kakushima, and H. Iwai, Appl. Phys. Express **6**, 91002 (2013).

[11] S. Takagi, A. Toriumi, M. Iwase, and H. Tango, IEEE Trans. Electron Devices **41**, 2357 (1994).

[12] G. Li, R. Wang, B. Song, J. Verma, Y. Cao, S. Ganguly, A. Verma, J. Guo, H.G. Xing, and D. Jena, IEEE Electron Device Lett. **34**, 852 (2013).

[13] R. Chu, Y. Cao, M. Chen, R. Li, and D. Zehnder, IEEE Electron Device Lett. **37**, 269 (2016).

[14] S. Kubota, R. Kayanuma, A. Nakajima, S. Nishizawa, and H. Ohashi, in *Mater. Res. Soc.* (Boston, Massachusetts, 2015), p. RR1.02.

[15] H. Hahn, B. Reuters, A. Pooth, B. Hollander, M. Heuken, H. Kalisch, and A. Vescan, IEEE Trans. Electron Devices **60**, 3005 (2013).

[16] A. Kumar and M.M. De Souza, in *2016 IEEE Int. Electron Devices Meet.* (IEDM, 2016), p. 7.4.1-7.4.4.

[17] A. Nakajima, S. Kubota, R. Kayanuma, K. Tsutsui, K. Kakushima, H. Wakabayashi, H. Iwai, S. Nishizawa, and H. Ohashi, in *13th Int. Semin. Power Semicond.* (2016).

[18] F.J. Kub, T.J. Anderson, A.D. Koehler, and K.D. Hobart, U.S. Patent No. 9,275,998 (6 August 2015).

[19] A. Kumar and M.M. De Souza, IET Power Electron. 3 (2017).

[20] A. Kumar and M.M. De Souza, IEEE Electron Device Lett. **38**, 1449 (2017).

[21] Silvaco TCAD Atlas, Version V3.44.1R, https://www.silvaco.com/products/tcad.html, accessed 19 March 2018.

[22] A. Nakajima, Y. Sumida, M.H. Dhyani, H. Kawai, and E.M.S. Narayanan, Appl. Phys. Express **3**, 121004 (2010).

[23] J. Chen and W.D. Brewer, Adv. Electron. Mater. **1**, 1500113 (2015).

[24] I.P. Smorchkova, E. Haus, B. Heying, P. Kozodoy, P. Fini, J.P. Ibbetson, S. Keller, S.P. DenBaars, J.S. Speck, and U.K. Mishra, Appl. Phys. Lett. **76**, 718 (2000).

[25] Bin Lu, Min Sun, and T. Palacios, IEEE Electron Device Lett. **34**, 369 (2013).

[26] Y. Ohmaki, M. Tanimoto, S. Akamatsu, and T. Mukai, Jpn. J. Appl. Phys. **45**, L1168 (2006).

List of Figures:

FIG. 1. Schematics of the p-channel E-mode device with AlGaN cap on top of a GaN channel, to deplete the 2DHG under the channel. In (a) the 2DEG is kept grounded along with the source (marked S) while in (b) the 2DEG is biased via an additional base contact (marked B).

FIG. 2. (a) Comparison of the simulated transfer characteristics with a variation in thickness of the GaN channel at a fixed threshold voltage of $-\boldsymbol{2}\ \boldsymbol{V}$ for a p-channel AlGaN capped device with grounded 2DEG. The inset shows the Al mole fraction in the AlGaN cap layer $\boldsymbol{x_{cap}}$ required to maintain the $\boldsymbol{V_{th}}$ at $-\boldsymbol{2}\ \boldsymbol{V}$ for different $\boldsymbol{t_{ch}}$ and the corresponding on-current. (b) Simulated Band diagrams at two different thicknesses of GaN channel.

FIG. 3. Simulated transfer characteristics at different base to source bias $\boldsymbol{V_B}$ applied to the 2DEG in the modified device in Figure 1 (b) for $\boldsymbol{30}\ \boldsymbol{nm}$ of channel thickness and $\boldsymbol{10}$ % of Al mole fraction in the AlGaN cap. The inset shows the corresponding on-current and threshold voltage behaviour with respect to $\boldsymbol{V_B}$.

FIG. 4. The simulated density of 2DHG in the gate and access regions with respect to a change in (a) Al mole fraction in AlGaN cap $\boldsymbol{x_{cap}}$ and (b) base voltage $\boldsymbol{V_B}$.

FIG. 5. The simulated transfer characteristics of an optimum device with a threshold voltage of $-2\ V$, featuring an AlGaN cap with Al mole fraction of 18 % at a potential of 3.45 V applied to the 2DEG. The inset shows the change in transfer characteristics due to a variation in trap charge at the interface between the regrown AlGaN cap and GaN channel.

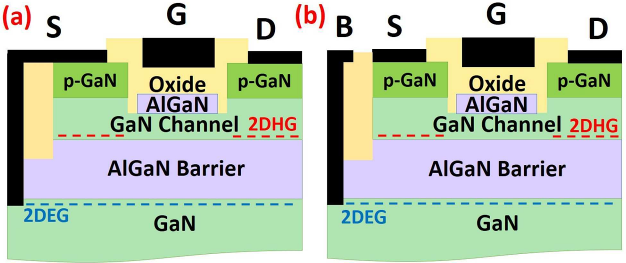
(a)
S
G
D
p-GaN
Oxide
p-GaN
AlGaN
GaN Channel
2DHG
AlGaN Barrier
2DEG
GaN
(b)
B
S
G
D
p-GaN
Oxide
p-GaN
AlGaN
GaN Channel
2DHG
AlGaN Barrier
2DEG
GaN

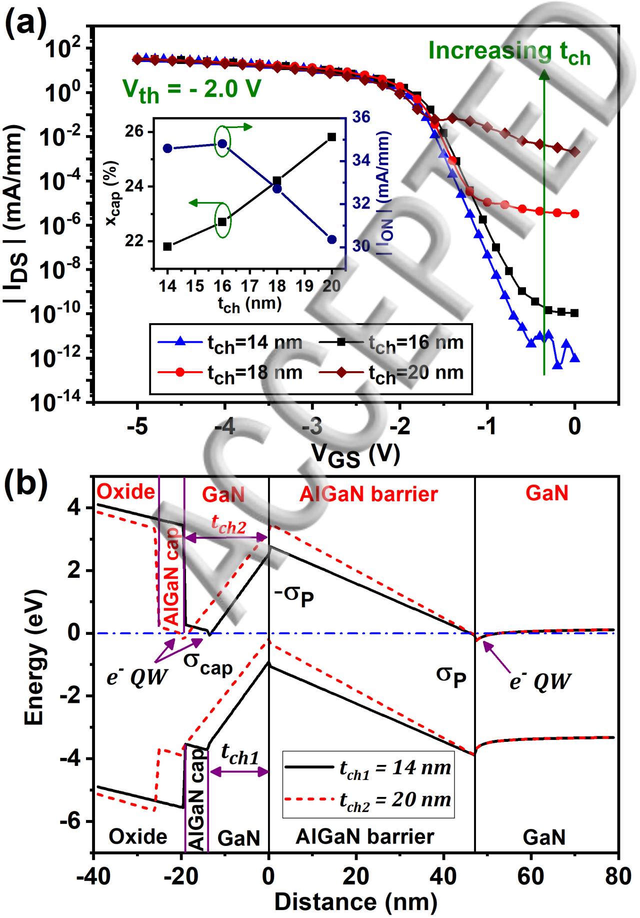
(a)
Increasing t_{ch}
V_{th} = - 2.0 V
$| I_{DS} |$ (mA/mm)
10^{2}
10^{0}
10^{-2}
10^{-4}
10^{-6}
10^{-8}
10^{-10}
10^{-12}
10^{-14}
x_{cap} (%)
26
24
22
36
34
32
30
$| I_{ON} |$ (mA/mm)
14 15 16 17 18 19 20
t_{ch} (nm)
t_{ch}=14 nm
t_{ch}=16 nm
t_{ch}=18 nm
t_{ch}=20 nm
-5 -4 -3 -2 -1 0
V_{GS} (V)
(b)
Oxide
GaN
AlGaN barrier
GaN
t_{ch2}
AlGaN cap
$-\sigma_P$
e^- QW
σ_{cap}
σ_P
e^- QW
t_{ch1}
AlGaN cap
t_{ch1} = 14 nm
t_{ch2} = 20 nm
Oxide
GaN
AlGaN barrier
GaN
Energy (eV)
4
2
0
-2
-4
-6
-40 -20 0 20 40 60 80
Distance (nm)

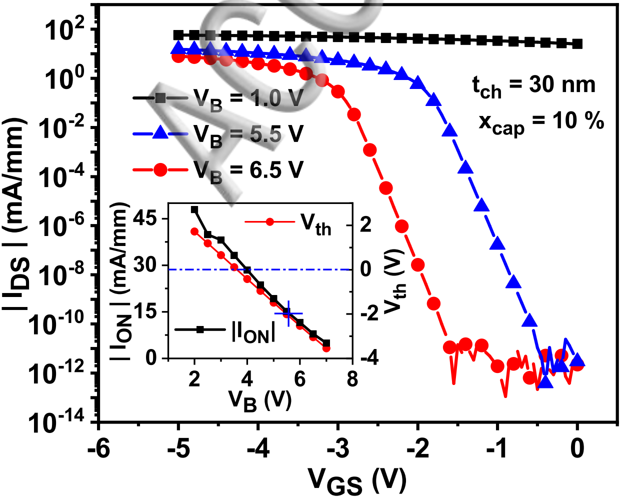
$|I_{DS}|$ (mA/mm)
V_{GS} (V)
10^{2}
10^{0}
10^{-2}
10^{-4}
10^{-6}
10^{-8}
10^{-10}
10^{-12}
10^{-14}
-6
-5
-4
-3
-2
-1
0
V_B = 1.0 V
V_B = 5.5 V
V_B = 6.5 V
t_{ch} = 30 nm
x_{cap} = 10 %
$|I_{ON}|$ (mA/mm)
V_{th} (V)
V_B (V)
V_{th}
$|I_{ON}|$
45
30
15
0
2
0
-2
-4
2
4
6
8

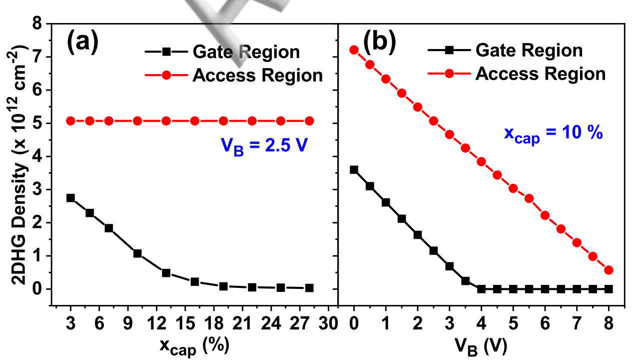
(a)
Gate Region
Access Region
$V_B = 2.5$ V
2DHG Density (x 10^{12} cm^{-2})
0
1
2
3
4
5
6
7
8
3
6
9
12
15
18
21
24
27
30
x_{cap} (%)
(b)
Gate Region
Access Region
$x_{cap} = 10$ %
0
1
2
3
4
5
6
7
8
V_B (V)

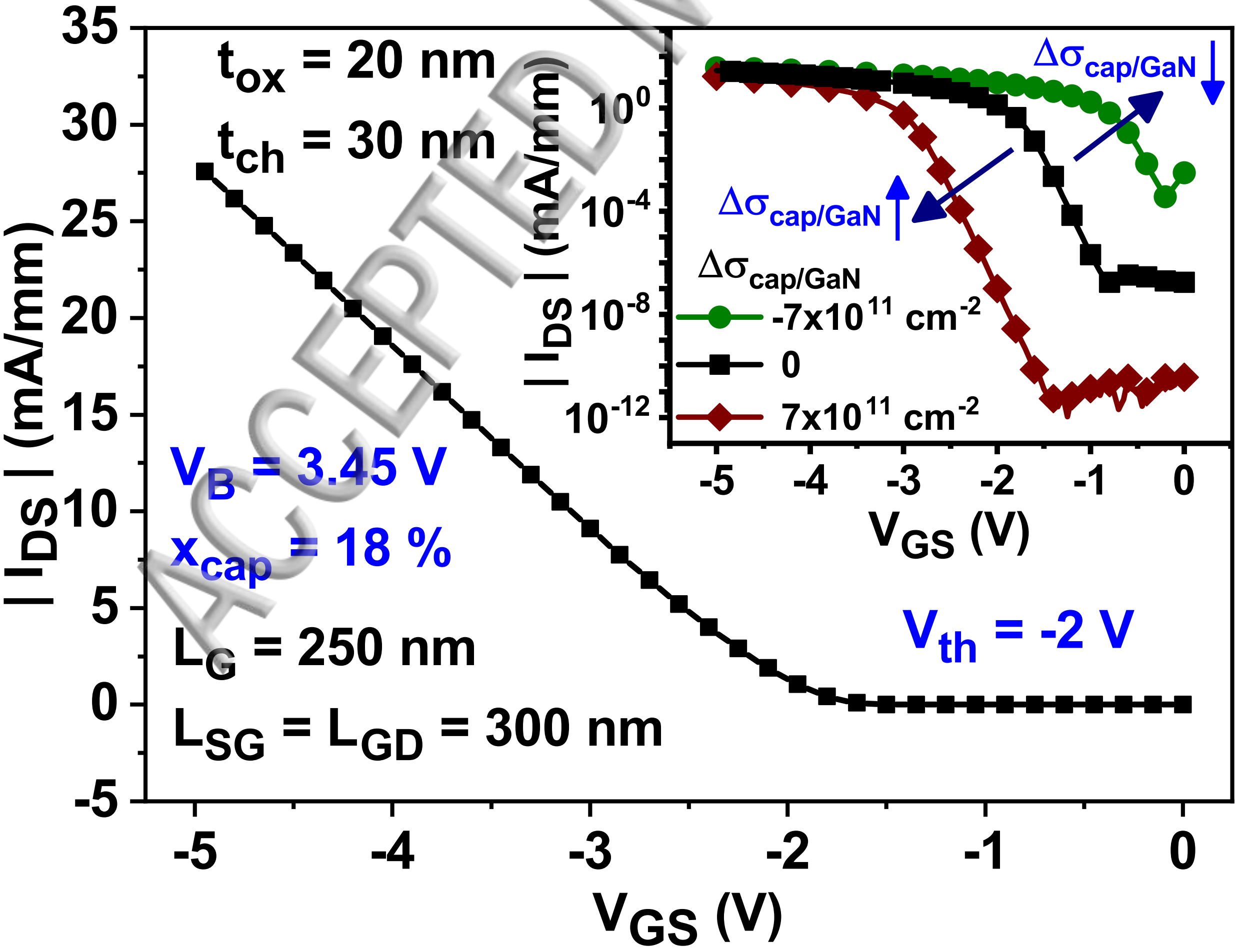

t_{ox} = 20 nm
t_{ch} = 30 nm
V_B = 3.45 V
x_{cap} = 18 %
L_G = 250 nm
L_{SG} = L_{GD} = 300 nm
V_{th} = -2 V
|I_{DS}| (mA/mm)
35
30
25
20
15
10
5
0
-5
-5
-4
-3
-2
-1
0
V_{GS} (V)
$\Delta\sigma_{cap/GaN}$
$\Delta\sigma_{cap/GaN}$
$\Delta\sigma_{cap/GaN}$
-7x10^{11} cm^{-2}
0
7x10^{11} cm^{-2}
|I_{DS}| (mA/mm)
10^0
10^{-4}
10^{-8}
10^{-12}
-5
-4
-3
-2
-1
0
V_{GS} (V)